Manuscript prepared for Biogeosciences Discuss.
with version 2015/04/24 7.83 Copernicus papers of the LaTeX class copernicus.cls.
Date: 21 March 2016

Non-deforestation fire vs. fossil fuel combustion: the source of CO_2 emissions affects the global carbon cycle and climate responses

J.-S. Landry[1,a] **and H. D. Matthews**[2]

[1]Department of Geography, McGill University, Montréal, Canada
[2]Department of Geography, Planning and Environment, Concordia University, Montréal, Canada
[a]currently at: the Department of Geography, Planning and Environment, Concordia University, Montréal, Canada

Correspondence to: J.-S. Landry (jean-sebastien.landry2@mail.mcgill.ca)

Abstract

Non-deforestation fire – i.e., fire that is typically followed by the recovery of natural vegetation – is arguably the most influential disturbance in terrestrial ecosystems, thereby playing a major role in carbon exchanges and affecting many climatic processes. The radiative effect from a given atmospheric CO_2 perturbation is the same for fire and fossil fuel combustion. However, major differences exist per unit of CO_2 emitted between the effects of non-deforestation fire vs. fossil fuel combustion on the global carbon cycle and climate, because: 1) fossil fuel combustion implies a net transfer of carbon from geological reservoirs to the atmospheric, oceanic, and terrestrial pools, whereas fire occurring in terrestrial ecosystems does not; 2) the average lifetime of the atmospheric CO_2 increase is longer when originating from fossil fuel combustion compared to fire, due to the strong vegetation regrowth following fire disturbances in terrestrial ecosystems; and 3) other impacts, for example on land surface albedo, also differ between fire and fossil fuel combustion. The main purpose of this study is to illustrate the consequences from these fundamental differences between fossil fuel combustion and non-deforestation fires using 1000-year simulations of a coupled climate–carbon model with interactive vegetation. We assessed emissions from both pulse and stable fire regime changes, considering both the gross (carbon released from combustion) and net (fire-caused change in land carbon, also accounting for vegetation decomposition and regrowth, as well as climate–carbon feedbacks) fire CO_2 emissions. In all cases, we found substantial differences from equivalent amounts of emissions produced by fossil fuel combustion. These findings suggest that side-by-side comparisons of non-deforestation fire and fossil fuel CO_2 emissions – implicitly implying that they have similar effects per unit of CO_2 emitted – should therefore be avoided, particularly when these comparisons involve gross fire emissions, because the reservoirs from which these emissions are drawn have very different residence times (millions of years for fossil fuel, years to centuries for vegetation and soil–litter). Our results also support the notion that most net emissions occur relatively soon after fire regime shifts and then progressively approach zero. Overall, our study calls for the explicit representation of fire activity as a valuable step

to foster a more accurate understanding of its impacts on global carbon cycling and temperature, compared to conceiving fire effects as congruent with the consequences from fossil fuel combustion.

1 Introduction

Fossil fuel combustion entails a net transfer of carbon from geological reservoirs to the much more active atmospheric, oceanic, and terrestrial carbon pools, thereby increasing the total amount of carbon in these pools and leading to an atmospheric CO_2 anomaly that decreases only gradually on a millennial timescale (Archer et al., 2009; Eby et al., 2009; Joos et al., 2013). This atmospheric CO_2 anomaly causes global warming that remains stable over thousands of years (Matthews and Caldeira, 2008; Eby et al., 2009; Clark et al., 2016). The atmospheric CO_2 anomaly also gives rise to a global CO_2 fertilization effect that decreases land surface albedo, due to dynamic vegetation expansion and generally higher vegetation cover; considered alone, this albedo decrease has a warming influence on the climate (Matthews, 2007; Bala et al., 2013).

Fire (also referred to as wildland fire, wildfire, biomass burning, and open vegetation burning) is a conspicuous disturbance in most terrestrial ecosystems, with considerable impacts on vegetation and climate (Bonan, 2008; Running, 2008; Bowman et al., 2009). Contrary to fossil fuel combustion, fire does not entail a net addition of CO_2 to the three active carbon pools of the Earth System, but simply redistributes the carbon already existing within these global pools. Except when used for permanent land clearing, fire usually triggers a strong local-scale vegetation regrowth response lasting years to decades depending upon the ecosystem (van der Werf et al., 2003; Goulden et al., 2011); hence the resulting atmospheric CO_2 anomaly and the concurrent global CO_2 fertilization are of shorter duration than after fossil fuel combustion. Fire also causes major modifications to land–atmosphere exchanges of energy through altered surface albedo and sensible/latent heat partitioning (Bremer and Ham, 1999; Amiro et al., 2006). Besides a short-term decrease due to surface blackening, local albedo generally increases after a fire event, thereby lead-

ing to a regional-scale cooling that is consequential at the global scale (Ward et al., 2012; Landry et al., 2015). For the same amount of emitted CO_2, fire therefore differs from fossil fuel combustion in terms of: 1) the net addition of CO_2 to the active carbon cycling pools for fossil fuel combustion only; 2) the average lifetime of the atmospheric CO_2 perturbation; and 3) the non-CO_2 climatic impacts (e.g., albedo) that also affect the carbon cycle. Given that these differences are in fact inseparable from the CO_2 emitting process, we expect the same amount of CO_2 emissions from fire vs. fossil fuel combustion to have different effects on the global carbon cycle and temperature. Variations in the amount and composition of aerosols emitted by the two processes also likely lead to further differences; unfortunately, even if fire-emitted aerosols might have a larger climatic impact than any other fire-caused effect, their exact forcing remains poorly constrained (Jacobson, 2004, 2014; Jones et al., 2007; Unger et al., 2010; Ward et al., 2012; Landry et al., 2015).

Fire currently affects around 300–500 $\mathrm{Mha\,yr^{-1}}$ (Mieville et al., 2010; Randerson et al., 2012; Giglio et al., 2013), leading to gross emissions (i.e., accounting only for the combustion of vegetation and soil–litter) of 1.5–3 $\mathrm{Pg\,C\,yr^{-1}}$ (Mieville et al., 2010; van der Werf et al., 2010; Randerson et al., 2012). The potential for modifications in the current fire regime to modulate climate change stimulated the explicit representation of fire in the Lund–Potsdam–Jena (LPJ) Dynamic Global Vegetation Model (DGVM; Thonicke et al., 2001), and later on into various other similar process-based models of climate–vegetation interactions (Arora and Boer, 2005; Kloster et al., 2010; Li et al., 2014). These efforts have paved the way to studies that projected an increase in fire activity and gross CO_2 emissions over the 21st century (Scholze et al., 2006; Pechony and Shindell, 2010; Kloster et al., 2012). The net effect of fire on global carbon cycling has however received less attention than the consequences from future changes in fire activity. In their seminal study, Seiler and Crutzen (1980) concluded that net biospheric emissions, coming mostly from fire, could range between $\pm 2\,\mathrm{Pg\,C\,yr^{-1}}$ by adding the effects of vegetation regrowth and other processes to their estimate of 2–4 $\mathrm{Pg\,C\,yr^{-1}}$ for gross fire emissions. The net effect of fire on global terrestrial carbon storage has then apparently been left unaddressed for more than three decades, until Ward et al. (2012) suggested a fire-caused net reduction of $\sim 500\,\mathrm{Pg\,C}$ in

pre-industrial land carbon. They also found that this reduction could currently be slightly lower (around 425 Pg C) due to offsetting effects between fire and land-use and land cover changes (LULCC), but could increase to about 550–650 Pg C by the end of this century due to a climate-driven increase in fire activity. More recently, Li et al. (2014) concluded that net fire emissions were equal to 1.0 Pg C yr^{-1} on average during the 20th century, compared to gross emissions of 1.9 Pg C yr^{-1} on average over the same period. While the fact that vegetation regrowth offsets a fraction of gross fire emissions has been appreciated for some time, previous global quantifications of the difference between gross and net emissions have been performed with first-order estimates (Seiler and Crutzen, 1980) or in offline terrestrial models (Ward et al., 2012; Li et al., 2014), and have neglected relevant processes. Indeed, net fire CO_2 emissions differ from gross emissions because they include not only the gradual decomposition of the non-trivial fraction of vegetation killed by fire but not combusted (especially for trees) and the post-fire vegetation regrowth, but also the effects of various feedbacks like the fire-induced CO_2 fertilization of terrestrial vegetation, or the impacts on vegetation productivity and soil–litter decomposition of temperature changes caused by modified atmospheric CO_2 and surface albedo.

In this study, we used a coupled climate–carbon model with interactive vegetation to advance the current knowledge regarding the effects of fire CO_2 emissions on the global carbon cycle and temperature. Using such a model allowed us to keep track of the total carbon in the Earth System, include the major role of the ocean in the fate of the fire-emitted CO_2, and account for the various feedbacks mentioned previously (i.e., CO_2 fertilization and temperature–CO_2 interactions), which are consequential for the global carbon cycle and temperature responses. We focussed on non-deforestation fires that allow the different vegetation types to compete and grow back in the recently burned area, because they constitute the bulk of global burned area and gross emissions (van der Werf et al., 2010) and have been much less represented in climate models than the LULCC events associated with deforestation fires. Our main objective is to compare the long-term effects of non-deforestation fire vs. fossil fuel combustion per unit of CO_2 emitted, for single fire pulses and stable fire regimes. A second objective is to quantify the differences between gross and

net fire CO_2 emissions over 1000 years following major changes in fire frequency; note that the simulated net emissions accounted for all processes mentioned previously (i.e., decomposition of fire-killed vegetation, regrowth, global CO_2 fertilization, and temperature–CO_2 interactions on land and in the ocean) in addition to the gross (i.e., combustion) emissions. To facilitate the interpretation of results, we performed all simulations against a background climate corresponding to pre-industrial conditions.

2 Methods

2.1 Modelling of fire and fossil fuel effects

We used the University of Victoria Earth System Climate Model (UVic ESCM) version 2.9 to study the climatic effects of fire and fossil fuel CO_2 emissions. The UVic ESCM computes at a resolution of $3.6^\circ \times 1.8^\circ$ (longitude $\times$ latitude) the exchanges of carbon, energy, and water among the land, atmosphere, and ocean (Weaver et al., 2001; Eby et al., 2009). The land module consists of a simplified version of the MOSES land surface scheme (Meissner et al., 2003) coupled to the TRIFFID DGVM (Cox, 2001). TRIFFID simulates the competition among five different plant functional types (PFTs): broadleaf tree, needleleaf tree, C_3 grass, C_4 grass, and shrub, accounting for the dynamics of different carbon pools for vegetation (leaves, stem, and roots) and soil–litter. The UVic ESCM computes the atmospheric energy and moisture balance with dynamical feedbacks, and its ocean module represents three-dimensional circulation, sea ice dynamics and thermodynamics, inorganic carbon, and ecosystem/biogeochemical exchanges (Weaver et al., 2001; Ewen et al., 2004; Schmittner et al., 2008; Eby et al., 2009).

The UVic ESCM can account for various types of prescribed forcings, including the emissions of CO_2, other greenhouse gases, and sulphate aerosols, land cover changes, volcanic aerosols, and land ice (Weaver et al., 2001; Matthews et al., 2004). In this study, we also used the UVic ESCM fire module developed by Landry et al. (2015). In each grid cell, this module estimated the gross CO_2 emissions coming from combustion as the product of pre-

scribed burned area (see Sect. 2.2), fuel density (simulated by the UVic ESCM), and PFT-specific combustion fractions for the different fuel types (Table 1). The carbon contained in the vegetation killed by fire but not combusted was transferred to the soil–litter pool, where it decomposed and released additional CO_2 at a rate that depended upon the simulated soil temperature and moisture. Since we were interested in non-deforestation fires, the different PFTs could compete and grow back in the recently burned area, giving rise to a regrowth CO_2 flux influenced by the climate–carbon feedbacks simulated by the UVic ESCM (e.g., fire-induced CO_2 fertilization and temperature changes). The model further accounted for the post-fire changes in land surface exchanges due to the modified vegetation cover, including the increase in land surface albedo (α_L, unitless). In all simulations, we included only the CO_2-related effects of fire and fossil fuel combustion, and not the associated aerosols and non-CO_2 greenhouse gases. We note that fire releases some carbon as carbon monoxide (CO) and methane (CH_4); however, these species constitute less than 10% of the fire-emitted carbon (Andreae and Merlet, 2001) and get mostly oxidized to CO_2 on a timescale shorter than the one of interest here (Ehhalt et al., 2001; Boucher et al., 2009). Similarly, we did not include here the short-term albedo decrease due to surface blackening.

2.2 Prescribed burned area

We based the prescribed burned area on the January 2001 to December 2012 monthly data from version 4 of the Global Fire Emissions Database (GFED4), which was derived from satellite observations (Giglio et al., 2013). We then simplified the GFED4 dataset in order to retain its most essential features only. Each grid cell from the UVic ESCM was labelled as a "fire cell" if it had been affected by fire at least once over the 2001–2012 period according to GFED4 (Fig. 1). The main simplification here was that the burned area fraction was set equal across all the UVic ESCM fire cells, with the specific burned area fraction value varying across fire simulations (see Sect. 2.3). The use of this binary distribution of burned area fractions (i.e., the same value for all fire cells and zero for all other cells) was necessary in order to reach the target fire CO_2 emissions while ensuring that the burned

area fractions were proportional for all fire cells across the different fire simulations. Given that the actual burned area fractions are already relatively close to 100 % in various regions (Giglio et al., 2013), upscaling the original GFED4 data would not have resulted in the same relative changes for all fire cells. Fire happened one time per year in each of the UVic ESCM fire cells, during the month of highest burned area according to the mean 2001–2012 value from GFED4 data (Fig. 1).

2.3 Simulation design

We started with an equilibrium run of the climate system for the year 1750, using the prescribed forcings from Eby et al. (2013) for solar radiation, atmospheric CO_2 (fixed at 277 ppmv), non-CO_2 greenhouse gases, land cover changes, land ice, and volcanic aerosols. Five groups of transient simulations then branched off from this equilibrated climate, in addition to a control transient simulation; in all cases, the forcings from year 1750 were maintained, except that the climate and carbon cycle were free to respond to the effects of the fire and fossil fuel experiments.

First, we performed three simulations that each consisted of a single year of fire activity, followed by a return towards the pre-fire equilibrium conditions. The resulting fire pulses had sizes of 20, 100, and 200 Pg C, based on their gross emissions (i.e., the carbon released from combustion only). We obtained these fire CO_2 pulses by adjusting the single-year burned area fraction across all fire cells and designate these simulations as Fire20P, Fire100P, and Fire200P.

Second, we performed another set of fire experiments similar to the previous ones, except that the same burned area fractions were maintained year after year. We designate these stable fire regimes as Fire20S, Fire100S, and Fire200S, corresponding to the previous fire pulse experiments of 20, 100, and 200 Pg C, respectively.

Third, we injected fossil fuel CO_2 pulses of 20, 100, and 200 Pg C into the atmosphere over a single year. The purpose of this set of three simulations was to compare the effects from fossil fuel CO_2 emissions vs. the same amount (and timing) of gross fire emissions. We designate these simulations as FF20P-G, FF100P-G, and FF200P-G.

Fourth, we wanted to compare the effects from fossil fuel CO_2 emissions vs. the same amount (and timing) of net fire emissions following each fire pulse. Each year, we computed the net fire emissions (land to atmosphere) as the annual change in total land carbon for the control simulation, minus the annual change in total land carbon following the fire pulse (Fire20P, Fire100P, or Fire200P). We then injected into the atmosphere yearly fossil fuel CO_2 emissions that were equal to these net fire emissions, including when they were negative (implying atmospheric carbon was sequestered back into geological reservoirs). We designate these simulations as FF20P-N, FF100P-N, and FF200P-N.

Fifth, we performed a set of three fossil fuel experiments in which the yearly fossil fuel CO_2 emissions were this time equal to the net emissions from the Fire20S, Fire100S, and Fire200S stable fire regimes. We designate this last set of simulations as FF20S-N, FF100S-N, FF200S-N.

3 Results

3.1 Assessment of the UVic ESCM fire module

The burned area fractions (unitless) in the fire cells for the 20, 100, and 200 Pg C pulses were approximately equal to 0.09, 0.45, and 0.88, respectively. Since the 200 Pg C pulse led to the burning of almost all the area within the fire cells, we used the results of this simulation to assess the post-fire simulated responses for changes in PFT cover, total biomass, and α_L in different ecosystem types (Fig. 2). In northern forests, the succession among the different PFTs (Fig. 2a) was qualitatively similar to, but noticeably slower than, observation-based trajectories (Rogers et al., 2013). Simulated fire-caused changes also appeared reasonable when compared with field observations for biomass (Fig. 2c) (Goulden et al., 2011) and α_L (Fig. 2e) (Amiro et al., 2006). As expected (van der Werf et al., 2003; Ward et al., 2012), the return to pre-fire conditions was much faster in savannas (Fig. 2b, d, and f). Note that the very small increase in total biomass soon after the fire pulse (Fig. 2d) and the associated

marginal decrease in α_L (Fig. 2f; not visible) likely came from the CO_2 fertilization effect caused by the long-lasting atmospheric CO_2 anomaly (see Sect. 3.2).

Additional simulations performed by Landry et al. (2015) further established the realism of results from the UVic ESCM fire module. First, they obtained gross fire CO_2 emissions of 2.2 Pg C yr^{-1} for the current fire regime, comparable to previous studies (Kloster et al., 2010; Mieville et al., 2010; Thonicke et al., 2010; van der Werf et al., 2010; Randerson et al., 2012; Li et al., 2014). The splitting of these gross emissions between vegetation (0.7 Pg C yr^{-1}) and soil–litter (1.5 Pg C yr^{-1}) also agreed with GFED-based estimates (van der Werf et al., 2010). Second, the differences in α_L between the current fire regime and a no-fire world simulated by Landry et al. (2015) led to a global radiative forcing of -0.11 W m^{-2} without the effect of surface blackening and -0.07 W m^{-2} with surface blackening, in agreement with observation-based estimates (Ward et al., 2012) (note that we did not include surface blackening in the current study).

3.2 Single fire pulse

The atmosphere, ocean, and land carbon pools responded as previously reported (Archer et al., 2009; Eby et al., 2009, 2013; Joos et al., 2013) to the fossil fuel CO_2 pulses (Fig. 3a). Part of the CO_2 injected into the atmosphere progressively became absorbed by the land and ocean, so that 1000 years after the pulses, 60 % of the additional CO_2 was taken up by the ocean and the remaining 40 % was divided almost equally between the land and atmosphere. The limited absolute difference among the pulse magnitudes studied here (i.e., 180 Pg C) explains why the responses were almost identical in the three cases, contrary to what has been found for a larger range of pulse magnitudes (Archer et al., 2009; Eby et al., 2009; Joos et al., 2013).

The results for fire (Fig. 3b) differed substantially from the fossil fuel pulse results. This time the CO_2 injected into the atmosphere came from the land, resulting in decreased land carbon rather than increased land carbon as in the case of fossil fuel. Instead of leading to long-lasting changes, the fire pulses were followed by a gradual return towards the initial equilibrium conditions. Moreover, the responses varied noticeably among the three fire

pulses. Finally, fractional changes greater than 1.0 were observed for the atmosphere and land shortly after the pulses because, due to the decomposition of the uncombusted vegetation killed by fire, the net emissions were higher than the gross emissions upon which the magnitude of the pulses were defined. Figure 3c compares the airborne fraction of the CO_2 pulses from fossil fuel vs. fire. All results were similar during ~ 25 years following the pulses, and for up to ~ 50 years for Fire100P and the different fossil fuel pulses. However, the airborne fraction became systematically higher for fossil fuel than for fire after about a century.

These differences then affected the global mean atmospheric surface temperature (T_s, in K), as shown in Fig. 4a. Fossil fuel CO_2 emission pulses caused relatively stable increases in T_s over millennial timescales (Matthews and Caldeira, 2008; Eby et al., 2009). In the case of fire pulses, the return of atmospheric CO_2 towards pre-fire levels (Fig. 3b) resulted in smaller warming of much shorter duration. Atmospheric CO_2 even decreased below the control level ~ 400–500 years after the pulses, which contributed to the observed long-term net cooling effect particularly visible for Fire200P. This slight decrease in atmospheric CO_2 came from the long time needed before the ocean returned to the atmosphere all the carbon absorbed following the fire pulses.

Albedo was also involved in the diverging effects of the two processes on T_s (Fig. 4b). Fossil fuel-induced CO_2 fertilization slightly decreased α_L (Matthews, 2007) over the whole simulation period, whereas fire noticeably increased α_L for decades to centuries. Note that contrary to the situation illustrated in Fig. 2a, in some northern grid cells tree cover had not fully recovered yet to pre-fire levels 1000 years after the 200 Pg C fire pulse. This lasting increase in α_L contributed to the net cooling following the fire pulses.

All previous outcomes illustrate that the effects on the global carbon cycle and temperature from fire vs. fossil fuel combustion differ for identical pulse magnitude defined in terms of gross (i.e., combustion only) fire emissions. Now, what if fossil fuel emissions were instead set equal to the net land-to-atmosphere emissions from fire year after year over the entire simulation, a situation where we expect fossil fuel combustion to better mimic the effects from fire? In this case, the impacts on land carbon remained opposite because

emissions came from the land for fire but not for fossil fuel; for the atmosphere, however, the CO_2 anomalies were more similar (Fig. 5a vs. Fig. 3b), though not identical as can be seen in Fig. 5b. During the first ~ 250 years, these anomalies were systematically lower for fossil fuel because the vegetation absorbed a portion of the emitted CO_2, whereas for fire the net emissions already accounted, by definition, for vegetation regrowth, global CO_2 fertilization, and all climate–carbon feedbacks. As a result, the ocean absorbed more carbon for fire than for fossil fuel emissions (Fig. 5a vs. Fig. 3b).

Based on atmospheric CO_2 alone, one would thus expect T_s to be higher for fire than for fossil fuels, yet the opposite was in fact observed (Fig. 5c) due to the opposite impacts on α_L (Fig. 5d). Note that in the long term, these ΔT_s were however much smaller than when fossil fuel emissions were equal to gross fire emissions (Fig. 4a). The fact that atmospheric CO_2 anomalies became slightly lower for fire than for fossil fuel after about 250 years (Fig. 5b; not visible) can be explained by long-lasting impacts on ocean carbon cycling: compared with fossil fuel, the ocean absorbed substantially more carbon in the initial decades after the fire pulses, and then took more time to outgas this carbon when the atmosphere–ocean fluxes shifted sign during the return towards the initial equilibrium conditions.

3.3 Stable fire regime

The previous results were based on single pulses of fire activity; we now turn to stable fire regimes for which the burned area fraction was maintained year after year, instead of being applied only once as in the pulse experiments. Figure 6 shows that the resulting gross and net emissions had qualitatively similar behaviours for the three stable regimes. Both the gross and net yearly emissions decreased quickly after an initial spike. The yearly net emissions progressively stabilized close to zero, although their mean value was still positive towards the end of the simulations as indicated by the slight positive slope of the cumulative net emissions. The yearly gross emissions, on the other hand, stabilized around much higher values because vegetation and soil–litter kept being combusted each year. Contrary to net emissions, the cumulative gross emissions thus increased almost linearly ~ 50 years after the onset of fire activity and onwards (results not shown).

Gross emissions thus appear highly inadequate to assess the cumulative impacts of fire regime shifts. Indeed, yearly gross emissions towards the end of the simulations were higher for Fire100S than for Fire200S, even though the outcome was obviously the opposite for the cumulative net emissions (Table 2). The lower land carbon density caused by more frequent fires has previously been reported to result in a "saturation effect" of gross emissions (Landry et al., 2015); here, this effect was so large that gross emissions ended up being lower for Fire200S than for Fire100S about 50 years after the onset of fire activity. A similar saturation effect clearly affected the cumulative net emissions, which were only twice as large for Fire200S compared to Fire20S, whereas the equilibrium yearly burned area was 12 times larger for Fire200S vs. Fire20S (Table 2). This slightly supra-linear scaling in burned area (e.g., 12 times instead of 10 times larger for Fire200S vs. Fire20S) among stable fire regimes was caused by fire-induced changes in vegetation composition. The input prescribed burned area in each fire cell (see Sect. 2.2) actually corresponds to a gross value that is reduced to account for the PFT-specific unburned islands occurring within burn perimeters (Kloster et al., 2010; van der Werf et al., 2010). More frequent fires led to increases in grass cover at the expense of trees and shrubs, thereby increasing the net burned area.

Even for fossil fuel emissions that were equal to the net emissions from stable fire regimes, the effects from the two processes differed once again. Figure 7a shows the distribution of net cumulative emissions (i.e., from year 0 until the specific year considered) from fossil fuel among the active carbon pools. This splitting was similar to the one following a single fossil fuel pulse (Fig. 3a), except that the maximum land uptake was proportionally lower and the ocean took a little longer to become the main carbon sink. For fire (Fig. 7b), land carbon rather decreased (with a fractional change equal to -1.0 as the net emissions were, by definition, equal to the total change in land carbon) and the uptake of carbon by the ocean had to be substantially higher than for fossil fuel.

The airborne fraction of the net emissions from stable fire regimes was initially higher than for the same amount of emissions from fossil fuel, but the anomalies in atmospheric CO_2 progressively became more similar (Fig. 8a). This should have caused T_s to be higher

for fire than for fossil fuel, yet once again the opposite was observed (Fig. 8b). Cumulative fossil fuel CO_2 emissions led to T_s increases that were relatively stable over thousands of years (Matthews and Caldeira, 2008; Eby et al., 2009). For fire, on the other hand, the initial increase in T_s after the onset of fire activity was followed $\sim$ 50–100 years later by a gradual decrease in T_s. As was the case for the pulse simulations (see Sect. 3.2), this different effect on T_s came from opposite changes in land albedo, which substantially increased for fire due to changes in vegetation cover, but slightly decreased for fossil fuel due to CO_2 fertilization (Fig. 8c).

4 Discussion

4.1 Fundamental differences between non-deforestation fire and fossil fuel combustion

In this study, we have shown a consistent pattern of fundamental differences between the effects on the carbon cycle and climate per unit of CO_2 emitted by non-deforestation fire vs. fossil fuel combustion. These discrepancies ultimately came from the net addition of CO_2 to the three active carbon pools by fossil fuel combustion (contrary to fire), as well as the differences in the average lifetime of the atmospheric CO_2 increase and in the non-CO_2 climatic impacts. First, the sources of CO_2 emissions are qualitatively distinct: fire simply reshuffles carbon among the active pools, whereas fossil fuel combustion entails a net carbon transfer from the geological to the active pools over millennial time scales (Archer et al., 2009; Eby et al., 2009). Second, the terrestrial pools (vegetation plus soil–litter) cannot respond in the same way to the atmospheric CO_2 anomalies created by fire vs. fossil fuel emissions. The only direct effect (i.e., excluding climate change) of fossil fuel emissions on land carbon storage occurs through the CO_2 fertilization effect. Fire, on the other hand, gives rise to a much more dynamic land carbon response. Fire activity not only leads to CO_2 emissions through the combustion of land carbon and the further decomposition of killed but uncombusted vegetation, but also decreases the amount of vegetation that can instantaneously be fertil-

ized by the fire-induced increase in atmospheric CO_2. Subsequently, however, vegetation regrowth and the associated soil–litter build up in the burned patches act as strong carbon sinks. Third, these contrasting effects on terrestrial vegetation mean opposite changes in land albedo: fire-induced decrease in vegetation cover increases α_L, whereas fossil fuel-induced CO_2 fertilization decreases α_L through dynamic vegetation changes like increased shrub and tree cover in tundra (Matthews, 2007) and generally higher leaf and stem area index for the vegetation already in place (Bala et al., 2013). This divergence in α_L responses implies unequal T_s changes, which then feed back to affect the carbon cycle itself. Therefore, the effects on carbon cycling and temperature are incongruent even when fossil fuel emissions are equal to the net emissions from fire.

Other variables than carbon pools and α_L were affected by these different changes in T_s and amplified them. Sea ice area, for example, often diverged noticeably between corresponding fossil fuel and fire simulations. For FF100P-G and FF200P-G, there was a small ($\sim 2\,\%$ and $\sim 4\,\%$, respectively) but permanent decrease in global sea ice area that did not occur in the corresponding fire simulations. For FF100P-N and FF200P-N, sea ice area also decreased a little for a few centuries at least before gradually returning toward initial levels. (For FF20P-G and FF20P-N, the changes in global sea ice area were indistinguishable from internal variability.) For fire pulses, on the other hand, the substantial $\Delta\alpha_L$-based cooling over the Northern Hemisphere due to extensive land masses slightly increased Arctic sea ice area; note that $\Delta\alpha_L$ had a much smaller absolute influence on Antarctic sea ice, for which the changes were highly variable spatially. Such transfer of α_L-induced cooling to the surrounding ocean has also been observed following deforestation simulations, along with an additional decrease in atmospheric temperature over most latitudes resulting from the lower ocean temperature (Davin and de Noblet-Ducoudré, 2010). In our simulations of stable fire regimes and the corresponding fossil fuel experiments, changes in sea ice area were much larger due to higher net CO_2 emissions. For fossil fuel, sea ice area was permanently reduced in all simulations. For fire, the $\Delta\alpha_L$-based cooling was not strong enough this time to prevent major losses of both Arctic and Antarctic sea ice, because the atmospheric CO_2 anomalies were larger and longer-lasting than following a single fire pulse. However, the in-

crease in α_L helped maintaining lower temperatures for the stable fire regimes than for the corresponding fossil fuel simulations, and global sea ice area progressively recovered to the control level, albeit with spatial differences between the Arctic and Antarctic that matched the hemispherical changes in atmospheric temperature.

4.2 Study limitations

The outcomes of our study should be interpreted with five caveats in mind. First, we developed idealized fire regimes in order to obtain substantial fire impacts while facilitating the comparison of results across the different magnitudes of pulses or stable regimes. Our fire regimes were therefore more severe than the current situation on Earth, as seen with our equilibrium results of $\geq 0.9\,\mathrm{Gha\,yr^{-1}}$ for burned area and $\geq 7.3\,\mathrm{Pg\,C\,yr^{-1}}$ for gross emissions under stable regimes (Table 2), vs. current values of 0.3–0.5 $\mathrm{Gha\,yr^{-1}}$ (Mieville et al., 2010; Randerson et al., 2012; Giglio et al., 2013) and 1.5–3 $\mathrm{Pg\,C\,yr^{-1}}$ (Mieville et al., 2010; van der Werf et al., 2010; Randerson et al., 2012), respectively. Moreover, our "equal" spatial fire patterns (i.e., same burned area fraction in each fire cell) gave much more weight to fires in extra-tropical regions compared with the current fire distribution (Giglio et al., 2013). Despite the differences in vegetation regrowth and fire-caused changes in albedo among regions, the impacts on atmospheric CO_2 and T_s did not seem overly sensitive to changes in the distribution of burned area fraction among fire cells following a single fire pulse (Fig. 9).

Second, we neglected all non-CO_2 emissions from fire and fossil fuel. Accounting for the short-term post-fire surface blackening caused by char would reduce the albedo cooling effect. On the other hand, explicitly tracking all the patches created by individual fire events, instead of representing their average grid-level effect as we did here, would increase the simulated albedo cooling effect over boreal forests at least (Landry et al., 2016), although the impact would likely be minor for the Fire200P and Fire200S simulations in which the burned area fraction was close to 90 % in each fire cell. Furthermore, the fire-caused emissions of aerosols and non-CO_2 greenhouse gases into the atmosphere would have a much stronger impact on T_s than changes in surface albedo; however, the magnitude and even the sign of the climatic effect from these non-CO_2 atmospheric emissions remain highly

uncertain (Jacobson, 2004, 2014; Jones et al., 2007; Unger et al., 2010; Ward et al., 2012; Landry et al., 2015). Future studies on the differences in the carbon cycling and temperature impacts between fire and fossil fuel would nevertheless benefit from considering the effects of non-CO_2 emissions.

Third, the UVic ESCM does not currently simulate the non-trivial exchanges of carbon between land and ocean (Regnier et al., 2013) or between inland waters and the atmosphere (Raymond et al., 2013), which are also impacted by fire. For example, the land-to-ocean flux of all particulate and dissolved pyrogenic carbon could be as high as ~ 50–$100\,\mathrm{Tg\,C\,yr^{-1}}$ (Bird et al., 2015). More research is therefore needed to accurately represent the highly variable and poorly quantified fate of such exchanges of pyrogenic carbon; meanwhile, their influence on our results is speculative, but is unlikely to challenge the main outcomes we obtained.

Fourth, the quantitative results we obtained were dependent upon the specific features of the UVic ESCM. For example, the simulated post-fire vegetation regrowth appeared too slow in northern grid cells (Fig. 2a), thereby overestimating the duration of both the α_L-based cooling and CO_2-based warming following fire. The carbon–concentration feedback parameters from the UVic ESCM are close to the mean from other fully coupled climate–carbon models, but its carbon–climate feedback parameters are on the high end (Arora et al., 2013), meaning that the atmospheric CO_2 levels were more affected by temperature changes than would have occurred in most other models. Once again, these factors should not challenge the main outcomes we obtained.

Fifth, our study addressed only non-deforestation fires after which the natural vegetation is free to recover. One might argue that our stable fire regimes are similar to deforestation fires because, over large spatial scales, both fire types decrease terrestrial carbon storage and vegetation cover. However, our non-deforestation fires affected equally all fire cells, whereas deforestation fires are deemed exclusive to tropical regions (van der Werf et al., 2010). Given that fire-induced changes in terrestrial carbon density and albedo vary substantially among regions, we caution against the direct extrapolation of our results to deforestation fires. In fact, when neglecting non-CO_2 emissions, deforestation fires are con-

ceptually more similar to other sources of LULCC than to non-deforestation fires. Note that previous global-scale climatic studies of LULCC (see Pongratz et al., 2014 for an extensive list) have represented all LULCC sources in the same way. Yet the variations in delayed CO_2 fluxes between fire and other LULCC sources matter for carbon cycling (Ramankutty et al., 2007; Houghton et al., 2012) and, as mentioned previously, non-CO_2 emissions could have a dominant impact on the climate. Consequently, studies dedicated to deforestation fires that specifically represent their delayed CO_2 fluxes and go beyond CO_2 emissions would allow for a more refined understanding of their climatic impacts.

5 Conclusions

The main purpose of this study was to illustrate the fundamental differences in the effects on the global carbon cycle and temperature resulting from the same amount of CO_2 emitted by non-deforestation fire vs. fossil fuel combustion. To do so, we simulated fire pulses and stable fire regimes of various magnitudes, as well as the corresponding fossil fuel emissions. The main outcomes we obtained were the following.

- The carbon sink stemming from vegetation regrowth led to widely diverging long-term impacts on the carbon cycle and temperature when fossil fuel emissions were equal to the gross emissions (i.e., based on combustion only) from a fire pulse, with the opposite changes in land surface albedo further compounding these discrepancies (Figs. 3 and 4). Side-by-side comparisons of gross fire CO_2 emissions to fossil fuel emissions are thus misleading and should be avoided.

- The impacts still differed, although much less severely, when fossil fuel emissions were equal to the net emissions following a fire pulse (Fig. 5). These results point towards the existence of irreconcilable disparities, per unit of CO_2 emitted, between the effects from fire vs. fossil fuel combustion.

– Obvious differences also arose when fossil fuel emissions were equal to the net emissions caused by stable fire regimes, particularly for land carbon, oceanic carbon, surface temperature, and land surface albedo (Figs. 7 and 8).

Our results also shed light on the evolution of gross vs. net fire emissions following fire regime changes. As expected, non-zero gross emissions were maintained indefinitely following a stable fire regime change, whereas most of the net emissions actually occurred relatively quickly after the regime shift and progressively decreased to almost zero (Fig. 6). Furthermore, a higher increase in fire frequency could result in lower equilibrium gross emissions due to the fire-induced decrease in the amount of fuel available (Table 2). Changes in gross emissions offered therefore a poor indicator of fire impacts on the carbon cycle.

Fire is arguably the most relevant disturbance in terrestrial ecosystems, with major impacts on carbon cycling and climate (Bonan, 2008; Running, 2008; Bowman et al., 2009). The overarching message from the present study is that fire effects cannot be obtained from, and should not be conceived as akin to, fossil fuel combustion – rather, fire deserves its own explicit representation in climate-related studies.

Author contributions. J.-S. Landry and H. D. Matthews designed the study, J.-S. Landry modified the UVic ESCM with advice from H. D. Matthews, J.-S. Landry performed the simulations and analyzed the results, J.-S. Landry prepared the manuscript with contributions from H. D. Matthews.

Acknowledgements. We want to thank Navin Ramankutty for helpful discussions about gross vs. net fire emissions. Comments from the two reviewers and the Editor helped us improve the manuscript. Funding was provided by a NSERC Discovery Grant to H. D. Matthews.

References

Amiro, B. D., Orchansky, A. L., Barr, A. G., Black, T. A., Chambers, S. D., Chapin, F. S., Goulden, M. L., Litvak, M., Liu, H. P., McCaughey, J. H., McMilland, A., and Randerson, J. T.: The effect of post-fire stand age on the boreal forest energy balance, Agr. Forest Meteorol., 140, 41–50, 2006.

Andreae, M. O. and Merlet, P.: Emission of trace gases and aerosols from biomass burning, Glob. Biogeochem. Cy., 15, 955–966, 2001.

Archer, D., Eby, M., Brovkin, V., Ridgwell, A., Cao, L., Mikolajewicz, U., Caldeira, K., Matsumoto, K., Munhoven, G., Montenegro, A., and Tokos, K.: Atmospheric lifetime of fossil fuel carbon dioxide, Annu. Rev. Earth Pl. Sc., 37, 117–134, 2009.

Arora, V. K. and Boer, G. J.: Fire as an interactive component of dynamic vegetation models, J. Geophys. Res. 110, G02008, doi:10.1029/2005JG000042, 2005.

Arora, V. K., Boer, G. J., Friedlingstein, P., Eby, M., Jones, C. D., Christian, J. R., Bonan, G., Bopp, L., Brovkin, V., Cadule, P., Hajima, T., Ilyina, T., Lindsay, K., Tjiputra, J. F., and Wu, T.: Carbon–concentration and carbon–climate feedbacks in CMIP5 Earth System Models, J. Climate, 26, 5289–5314, 2013.

Bala, G., Krishna, S., Narayanappa, D., Cao, L., Caldeira, K., and Nemani, R.: An estimate of equilibrium sensitivity of global terrestrial carbon cycle using NCAR CCSM4, Clim. Dynam., 40, 1671–1686, 2013.

Bird, M. I., Wynn, J. G., Saiz, G., Wurster, C. M., and McBeath, A.: The pyrogenic carbon cycle, Annu. Rev. Earth Pl. Sc., 43, 273–298, 2015.

Bonan, G. B.: Forests and climate change: forcings, feedbacks, and the climate benefits of forests, Science, 320, 1444–1449, 2008.

Boucher, O., Friedlingstein, P., Collins, B., Shine, K. P.: The indirect global warming potential and global temperature change potential due to methane oxidation. Environ. Res. Lett., 4, 44007, doi:10.1088/1748-9326/4/4/044007, 2009.

Bowman, D. M. J. S., Balch, J. K., Artaxo, P., Bond, W. J., Carlson, J. M., Cochrane, M. A., D'Antonio, C. M., DeFries, R. S., Doyle, J. C., Harrison, S. P., Johnston, F. H., Keeley, J. E., Krawchuk, M. A., Kull, C. A., Marston, J. B., Moritz, M. A., Prentice, I. C., Roos, C. I., Scott, A. C., Swetnam, T. W., van der Werf, G. R., and Pyne, S. J.: Fire in the Earth system, Science, 324, 481–484, 2009.

Bremer, D. J. and Ham, J. M.: Effect of spring burning on the surface energy balance in a tallgrass prairie, Agr. Forest Meteorol., 97, 43–54, 1999.

Clark, P. U., Shakun, J. D., Marcott, S. A., Mix, A. C., Eby, M., Kulp, S., Levermann, A., Milne, G. A., Pfister, P. L., Santer, B. D., Schrag, D. P., Solomon, S., Stocker, T. F., Strauss, B. H., Weaver, A. J., Winkelmann, R., Archer, D., Bard, E., Goldner, A., Lambeck, K., Pierrehumbert, R. T., Plattner, G.-K.: Consequences of twenty-first-century policy for multi-millennial climate and sea-level change, Nature Climate Change, doi:10.1038/NCLIMATE2923, 2016.

Cox, P. M.: Description of the "TRIFFID" Dynamic Global Vegetation Model, Hadley Centre technical note 24, Hadley Centre, Met Office, UK, available at: http://www.metoffice.gov.uk/media/pdf/9/h/HCTN_24.pdf (last access: 10 September 2015), 16 pp., 2001.

Davin, E. L., and de Noblet-Ducoudré, N.: Climatic impact of global-scale deforestation: radiative versus nonradiative processes, J. Climate, 23, 97–112, 2010.

Eby, M., Zickfeld, K., Montenegro, A., Archer, D., Meissner, K. J., and Weaver, A. J.: Lifetime of anthropogenic climate change: millennial time scales of potential CO_2 and surface temperature perturbations, J. Climate, 22, 2501–2511, 2009.

Eby, M., Weaver, A. J., Alexander, K., Zickfeld, K., Abe-Ouchi, A., Cimatoribus, A. A., Crespin, E., Drijfhout, S. S., Edwards, N. R., Eliseev, A. V., Feulner, G., Fichefet, T., Forest, C. E., Goosse, H., Holden, P. B., Joos, F., Kawamiya, M., Kicklighter, D., Kienert, H., Matsumoto, K., Mokhov, I. I., Monier, E., Olsen, S. M., Pedersen, J. O. P., Perrette, M., Philippon-Berthier, G., Ridgwell, A., Schlosser, A., Schneider von Deimling, T., Shaffer, G., Smith, R. S., Spahni, R., Sokolov, A. P., Steinacher, M., Tachiiri, K., Tokos, K., Yoshimori, M., Zeng, N., and Zhao, F.: Historical and idealized climate model experiments: an intercomparison of Earth system models of intermediate complexity, Clim. Past, 9, 1111–1140, doi:10.5194/cp-9-1111-2013, 2013.

Ehhalt, D., Prather, M., Dentener, F., Derwent, R., Dlugokencky, E., Holland, E., Isaksen, I., Katima, J., Kirchhoff, V., Matson, P., Midgley, P., and Wang, M. Atmospheric chemistry and greenhouse gases. In: Houghton, J. T., Ding, Y., Griggs, D. J., Noguer, M., van der Linden, P. J., Dai, X., Maskell, K., and Johnson, C. A. (Eds.), Climate Change 2001: The Scientific Basis. Cambridge University Press, Cambridge, UK, pp. 239–288, 2001.

Ewen, T. L., Weaver, A. J., and Eby, M.: Sensitivity of the inorganic ocean carbon cycle to future climate warming in the UVic coupled model, Atmos. Ocean, 42, 23–42, 2004.

Giglio, L., Randerson, J. T., and van der Werf, G. R.: Analysis of daily, monthly, and annual burned area using the fourth-generation global fire emissions database (GFED4), J. Geophys. Res., 118, 317–328, 2013.

Goulden, M. L., McMillan, A. M. S., Winston, G. C., Rocha, A. V., Manies, K. L., Harden, J. W., and Bond-Lamberty, B. P.: Patterns of NPP, GPP, respiration, and NEP during boreal forest succession, Glob. Change Biol., 17, 855–871, 2011.

Houghton, R. A., House, J. I., Pongratz, J., van der Werf, G. R., DeFries, R. S., Hansen, M. C., Le Quéré, C., and Ramankutty, N.: Carbon emissions from land use and land-cover change, Biogeosciences, 9, 5125–5142, doi:10.5194/bg-9-5125-2012, 2012.

Jacobson, M. Z.: The short-term cooling but long-term global warming due to biomass burning, J. Climate, 17, 2909–2926, 2004.

Jacobson, M. Z.: Effect of biomass burning on climate, accounting for heat and moisture fluxes, black and brown carbon, and cloud absorption effects, J. Geophys. Res.-Atmos., 119, 8980–9002, 2014.

Jones, A., Haywood, J. M., and Boucher, O.: Aerosol forcing, climate response and climate sensitivity in the Hadley Centre climate model, J. Geophys. Res., 112, D20211, doi:10.1029/2007JD008688, 2007.

Joos, F., Roth, R., Fuglestvedt, J. S., Peters, G. P., Enting, I. G., von Bloh, W., Brovkin, V., Burke, E. J., Eby, M., Edwards, N. R., Friedrich, T., Frölicher, T. L., Halloran, P. R., Holden, P. B., Jones, C., Kleinen, T., Mackenzie, F. T., Matsumoto, K., Meinshausen, M., Plattner, G.-K., Reisinger, A., Segschneider, J., Shaffer, G., Steinacher, M., Strassmann, K., Tanaka, K., Timmermann, A., and Weaver, A. J.: Carbon dioxide and climate impulse response functions for the computation of greenhouse gas metrics: a multi-model analysis, Atmos. Chem. Phys., 13, 2793–2825, doi:10.5194/acp-13-2793-2013, 2013.

Kloster, S., Mahowald, N. M., Randerson, J. T., Thornton, P. E., Hoffman, F. M., Levis, S., Lawrence, P. J., Feddema, J. J., Oleson, K. W., and Lawrence, D. M.: Fire dynamics during the 20th century simulated by the Community Land Model, Biogeosciences, 7, 1877–1902, doi:10.5194/bg-7-1877-2010, 2010.

Kloster, S., Mahowald, N. M., Randerson, J. T., and Lawrence, P. J.: The impacts of climate, land use, and demography on fires during the 21st century simulated by CLM-CN, Biogeosciences, 9, 509–525, doi:10.5194/bg-9-509-2012, 2012.

Landry, J.-S., Matthews, H. D., and Ramankutty, N.: A global assessment of the carbon cycle and temperature responses to major changes in future fire regime, Climatic Change, 133, 179–192, 2015.

Landry, J.-S., Ramankutty, N., and Parrott, L.: Investigating the effects of sub-grid cell dynamic heterogeneity on the large-scale modelling of albedo in boreal forests, Earth Interact., 20, doi:10.1175/EI-D-15-0022.1, 2016.

Li, F., Bond-Lamberty, B., and Levis, S.: Quantifying the role of fire in the Earth system – Part 2: Impact on the net carbon balance of global terrestrial ecosystems for the 20th century, Biogeosciences, 11, 1345–1360, doi:10.5194/bg-11-1345-2014, 2014.

Matthews, H. D.: Implications of CO_2 fertilization for future climate change in a coupled climate–carbon model, Glob. Change Biol., 13, 1068–1078, 2007.

Matthews, H. D. and Caldeira, K.: Stabilizing climate requires near-zero emissions, Geophys. Res. Lett., 35, L04705, doi:10.1029/2007GL032388, 2008.

Matthews, H. D., Weaver, A. J., Meissner, K. J., Gillett, N. P., and Eby, M.: Natural and anthropogenic climate change: incorporating historical land cover change, vegetation dynamics and the global carbon cycle, Clim. Dynam., 22, 461–479, 2004.

Meissner, K. J., Weaver, A. J., Matthews, H. D., and Cox, P. M.: The role of land surface dynamics in glacial inception: a study with the UVic Earth System Model, Clim. Dynam., 21, 515–537, 2003.

Mieville, A., Granier, C., Liousse, C., Guillaume, B., Mouillot, F., Lamarque, J.-F., Grégoire, J.-M., and Pétron, G.: Emissions of gases and particles from biomass burning during the 20th century using satellite data and an historical reconstruction, Atmos. Environ., 44, 1469–1477, 2010.

Pechony, O. and Shindell, D. T.: Driving forces of global wildfires over the past millennium and the forthcoming century, P. Natl. Acad. Sci. USA, 107, 19167–19170, 2010.

Pongratz, J., Reick, C. H., Houghton, R. A., and House, J. I.: Terminology as a key uncertainty in net land use and land cover change carbon flux estimates, Earth Syst. Dynam., 5, 177–195, doi:10.5194/esd-5-177-2014, 2014.

Ramankutty, N., Gibbs, H. K., Achard, F., DeFries, R., Foley, J. A., and Houghton, R. A.: Challenges to estimating carbon emissions from tropical deforestation, Glob. Change Biol., 13, 51–66, 2007.

Randerson, J. T., Chen, Y., van der Werf, G. R., Rogers, B. M., and Morton, D. C.: Global burned area and biomass burning emissions from small fires, J. Geophys. Res., 117, G04012, doi:10.1029/2012JG002128, 2012.

Raymond, P. A., Hartmann, J., Lauerwald, R., Sobek, S., McDonald, C., Hoover, M., Butman, D., Striegl, R., Mayorga, E., Humborg, C., Kortelainen, P., Dürr, H., Meybeck, M., Ciais, P., and Guth, P.: Global carbon dioxide emissions from inland waters, Nature, 503, 355–359, 2013.

Regnier, P., Friedlingstein, P., Ciais, P., Mackenzie, F. T., Gruber, N., Janssens, I. A., Laruelle, G. G., Lauerwald, R., Luyssaert, S., Andersson, A. J., Arndt, S., Arnosti, C., Borges, A. V., Dale, A. W., Gallego-Sala, A., Goddéris, Y., Goossens, N., Hartmann, J., Heinze, C., Ilyina, T., Joos, F., LaRowe, D. E., Leifeld, J., Meysman, F. J. R., Munhoven, G., Raymond, P. A., Spahni, R., Suntharalingam, P., and Thullner, M.: Anthropogenic perturbation of the carbon fluxes from land to ocean, Nat. Geosci., 6, 597–607, 2013.

Rogers, B. M., Randerson, J. T., and Bonan, G. B.: High-latitude cooling associated with landscape changes from North American boreal forest fires, Biogeosciences, 10, 699–718, doi:10.5194/bg-10-699-2013, 2013.

Running, S. W.: Ecosystem disturbance, carbon, and climate, Science, 321, 652–653, 2008.

Schmittner, A., Oschlies, A., Matthews, H. D., and Galbraith, E. D.: Future changes in climate, ocean circulation, ecosystems, and biogeochemical cycling simulated for a business-as-usual CO_2 emission scenario until year 4000 AD, Global Biogeochem. Cy., 22, GB1013, doi:10.1029/2007GB002953, 2008.

Scholze, M., Knorr, W., Arnell, N. W., and Prentice, I. C.: A climate-change risk analysis for world ecosystems, P. Natl. Acad. Sci. USA, 103, 13116–13120, 2006.

Seiler, W. and Crutzen, P. J.: Estimates of gross and net fluxes of carbon between the biosphere and the atmosphere from biomass burning, Climatic Change, 2, 207–247, 1980.

Thonicke, K., Venevsky, S., Sitch, S., and Cramer, W.: The role of fire disturbance for global vegetation dynamics: coupling fire into a Dynamic Global Vegetation Model, Global Ecol. Biogeogr., 10, 661–677, 2001.

Thonicke, K., Spessa, A., Prentice, I. C., Harrison, S. P., Dong, L., and Carmona-Moreno, C.: The influence of vegetation, fire spread and fire behaviour on biomass burning and trace gas emissions: results from a process-based model, Biogeosciences, 7, 1991–2011, doi:10.5194/bg-7-1991-2010, 2010.

Unger, N., Bond, T. C., Wang, J. S., Koch, D. M., Menon, S., Shindell, D. T., and Bauer, S.: Attribution of climate forcing to economic sectors, P. Natl. Acad. Sci. USA, 107, 3382–3387, 2010.

van der Werf, G. R., Randerson, J. T., Collatz, G. J., and Giglio, L.: Carbon emissions from fires in tropical and subtropical ecosystems, Glob. Change Biol., 9, 547–562, 2003.

van der Werf, G. R., Randerson, J. T., Giglio, L., Collatz, G. J., Mu, M., Kasibhatla, P. S., Morton, D. C., DeFries, R. S., Jin, Y., and van Leeuwen, T. T.: Global fire emissions and the contribution of deforestation, savanna, forest, agricultural, and peat fires (1997–2009), Atmos. Chem. Phys., 10, 11707–11735, doi:10.5194/acp-10-11707-2010, 2010.

Ward, D. S., Kloster, S., Mahowald, N. M., Rogers, B. M., Randerson, J. T., and Hess, P. G.: The changing radiative forcing of fires: global model estimates for past, present and future, Atmos. Chem. Phys., 12, 10857–10886, doi:10.5194/acp-12-10857-2012, 2012.

Weaver, A. J., Eby, M., Wiebe, E. C., Bitz, C. M., Duffy, P. B., Ewen, T. L., Fanning, A. F., Holland, M. M., MacFadyen, A., Matthews, H. D., Meissner, K. J., Saenko, O., Schmittner, A., Wang, H., and Yoshimori, M.: The UVic earth system climate model: model description, climatology, and applications to past, present and future climates, Atmos. Ocean, 39, 361–428, 2001.

Table 1. Combustion fractions (all unitless) for the different PFTs (BT = broadleaf tree; NT = needleleaf tree; C3G = C_3 grass; C4G = C_4 grass; SH = shrub) and temporarily unvegetated portion of the grid cell (UNVEG). n/a: not applicable.

Fuel type	BT	NT	C3G	C4G	SH	UNVEG
PFT stem	0.30	0.30	0.95	0.95	0.30	n/a
PFT leaves	0.90	0.90	0.95	0.95	0.90	n/a
PFT roots	0.00	0.00	0.00	0.00	0.00	n/a
Soil–litter	0.12	0.12	0.05	0.05	0.10	0.05*

* The unvegetated fraction can be affected by fire only when the prescribed burned area is greater than the area covered by the five PFTs.

Table 2. Burned area and emissions* for the three stable fire regimes.

Regime	Burned area ($Gha\,yr^{-1}$)	Gross emissions ($Pg\,C\,yr^{-1}$)	Cumulative net emissions ($Pg\,C$)
Fire20S	0.9	7.3	629
Fire100S	5.4	21.1	966
Fire200S	10.8	18.9	1338

* Yearly results are the mean values over the last 60 years of simulation, whereas the cumulative net emissions are for the entire simulation. The onset of fire activity happened on year 0, after which fire frequency remained constant.

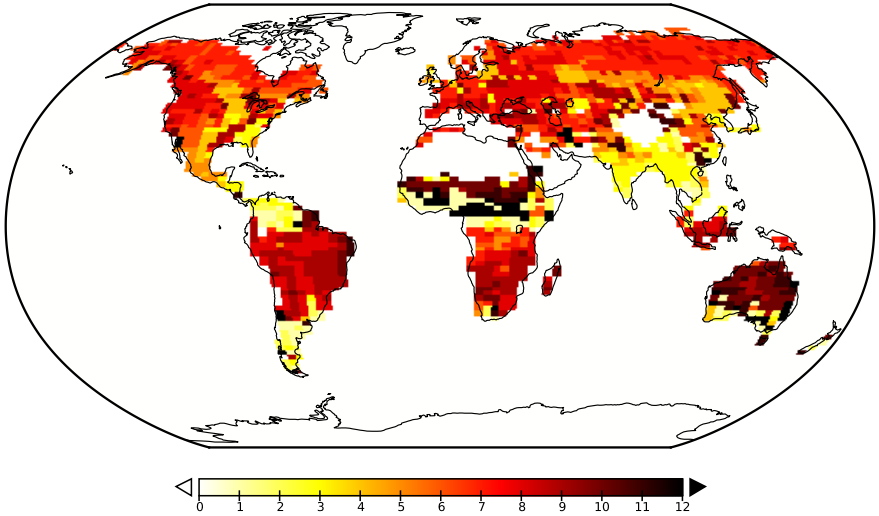

Figure 1. “Fire cells” used in the fire simulations. Numbers from 1 to 12 give the month of the year when fire occurs, whereas number 0 corresponds to grid cells without fire.

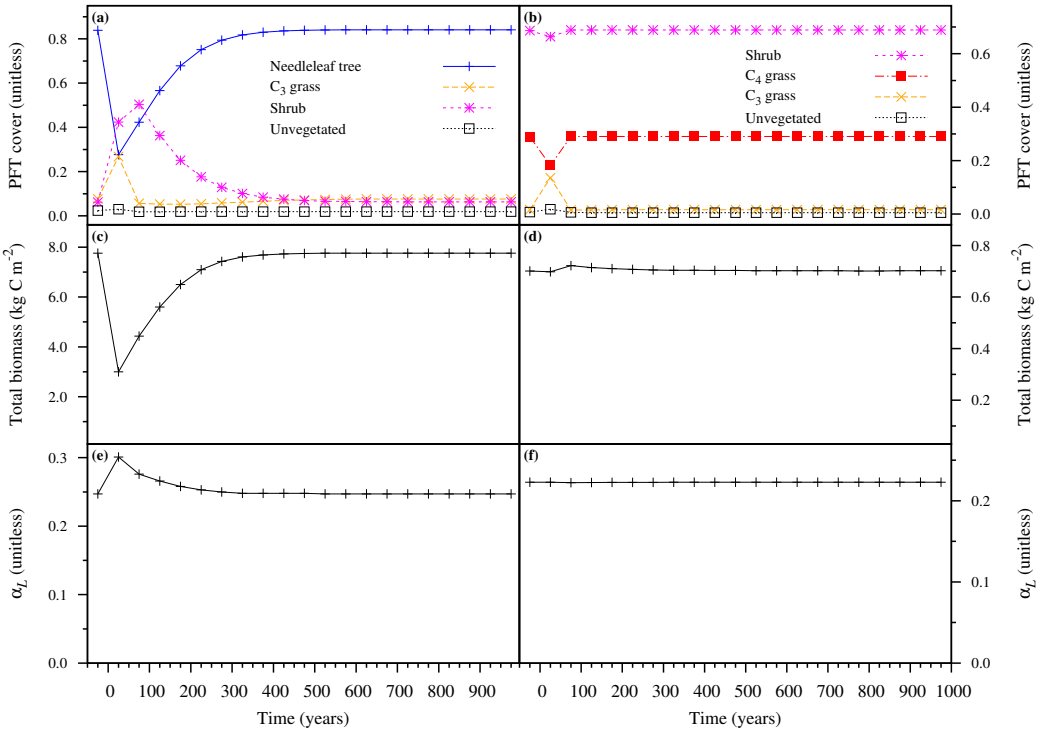

Figure 2. Changes due to the 200 Pg C fire pulse happening on year zero; each data point gives the mean value over 50 years (25 years before and 25 years after). Results are for a forested grid cell in North America (centered on 53.1° N, 124.2° W; panels **a**, **c**, and **e**) and a savanna grid cell in Africa (centered on 13.5° N, 12.6° E; panels **b**, **d**, and **f**). **(a, b)** Fractional cover of the different plant functional types. **(c, d)** Total biomass. **(e, f)** Land surface albedo.

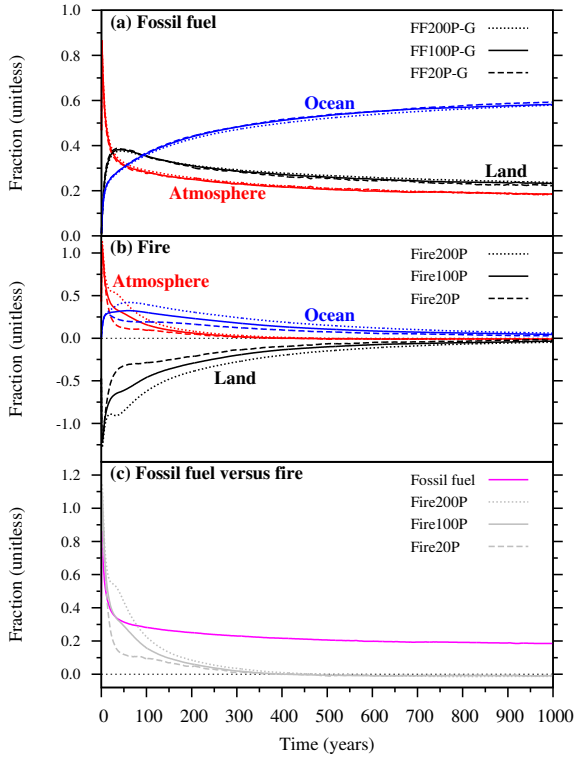

Figure 3. Changes in global carbon stocks resulting from the pulse experiments, expressed as fractions of each pulse magnitude. **(a)** Fossil fuel pulses, which were set equal to gross fire emissions. **(b)** Fire pulses. The fractions were sometimes greater than 1.0 for the atmosphere and land, because pulses were defined based on direct combustion only. **(c)** Results for atmospheric carbon only (i.e., airborne fraction); for fossil fuel, only FF100P-G is illustrated as the results were almost equal for the FF20P-G and FF200P-G cases (see panel **a**).

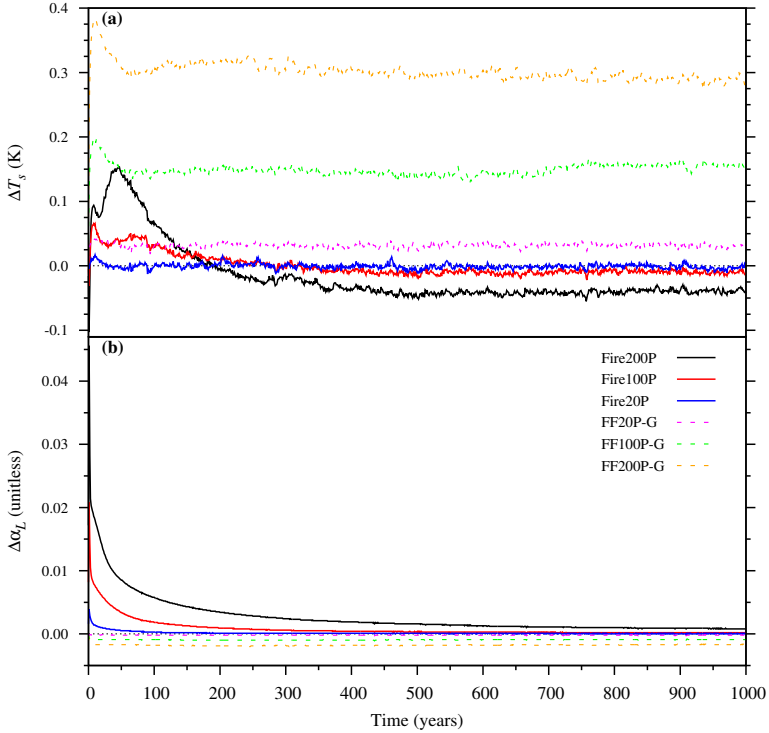

Figure 4. Changes in **(a)** global mean atmospheric surface temperature and **(b)** global mean land surface albedo from the pulse experiments. The fossil fuel emissions were set equal to gross fire emissions.

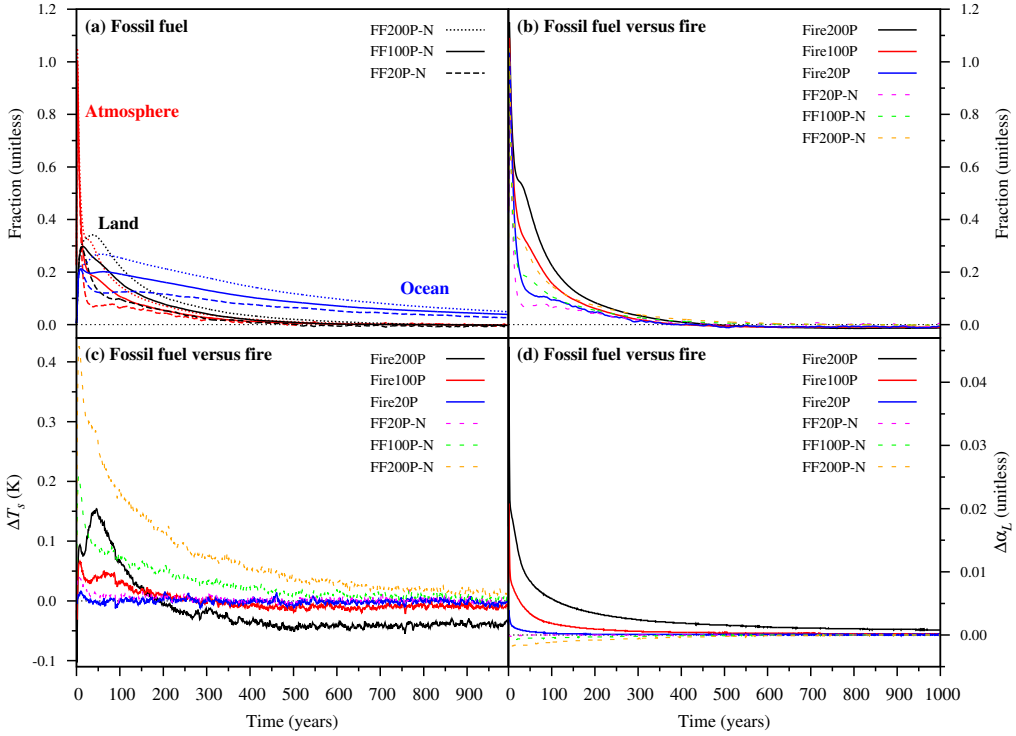

Figure 5. Effect of fossil fuel emissions set equal to net fire emissions. **(a)** Changes in global carbon stocks, expressed as fractions of each fire pulse magnitude. **(b)** Comparison with fire for the total atmospheric carbon, expressed as a fraction of each fire pulse magnitude. **(c)** Comparison with fire for the global mean atmospheric surface temperature. **(d)** Comparison with fire for the global mean land surface albedo.

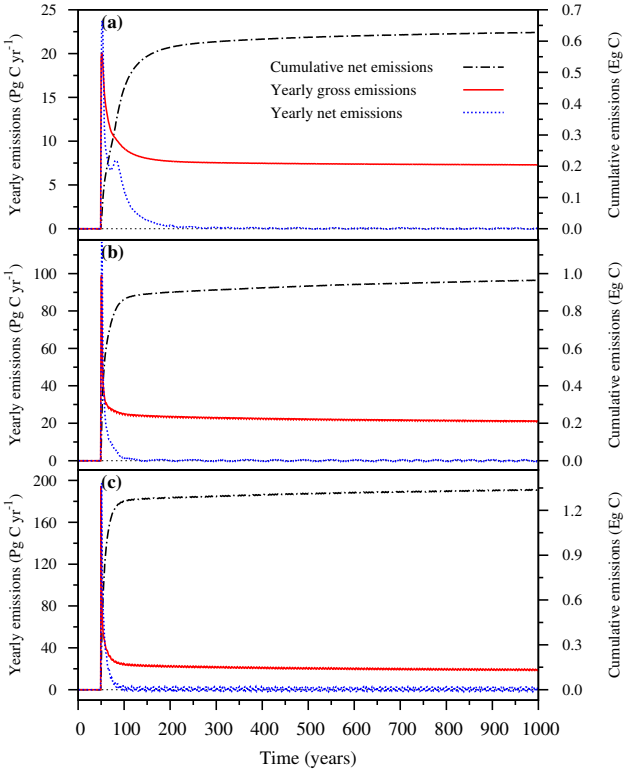

Figure 6. Yearly (both gross and net; left axis) and cumulative (right axis; 1 Eg C = 1000 Pg C) carbon emissions for the stable fire regimes. The onset of fire activity happened on year 0, after which fire frequency remained constant. **(a)** Fire20S. **(b)** Fire100S. **(c)** Fire200S.

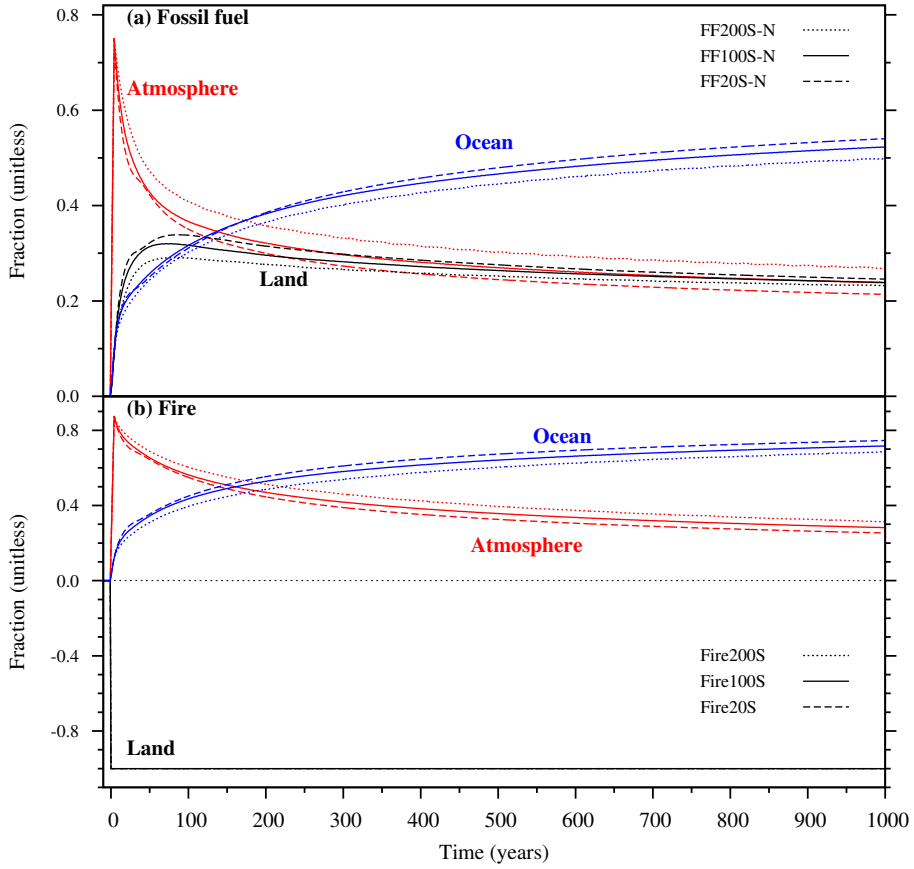

Figure 7. Changes in global carbon stocks resulting from the stable regime experiments. The changes are expressed as fractions of net cumulative emissions until the specific year considered. **(a)** Fossil fuel emissions, which were set equal to net yearly fire emissions. **(b)** Stable fire regimes; the onset of fire activity happened on year 0, after which fire frequency remained constant.

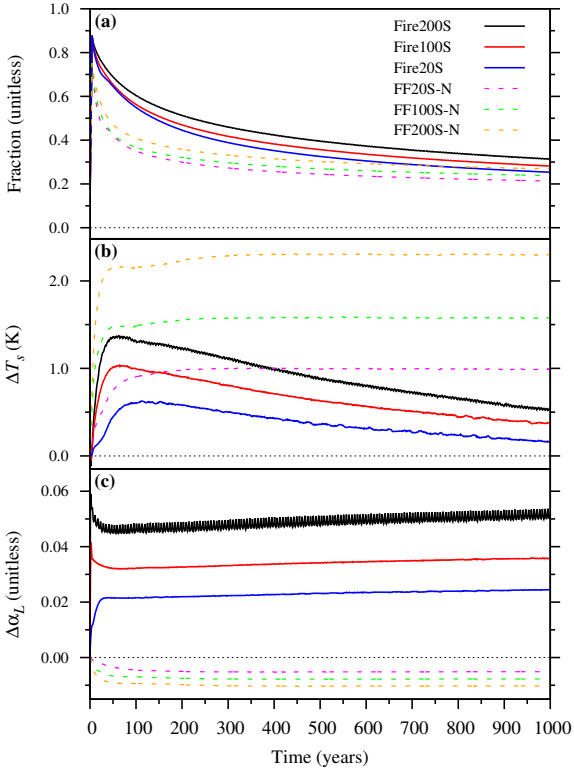

Figure 8. Changes in **(a)** atmospheric fraction of net cumulative emissions, **(b)** global mean atmospheric surface temperature, and **(c)** global mean land surface albedo from the stable regime experiments. The fossil fuel emissions were set equal to net yearly fire emissions.

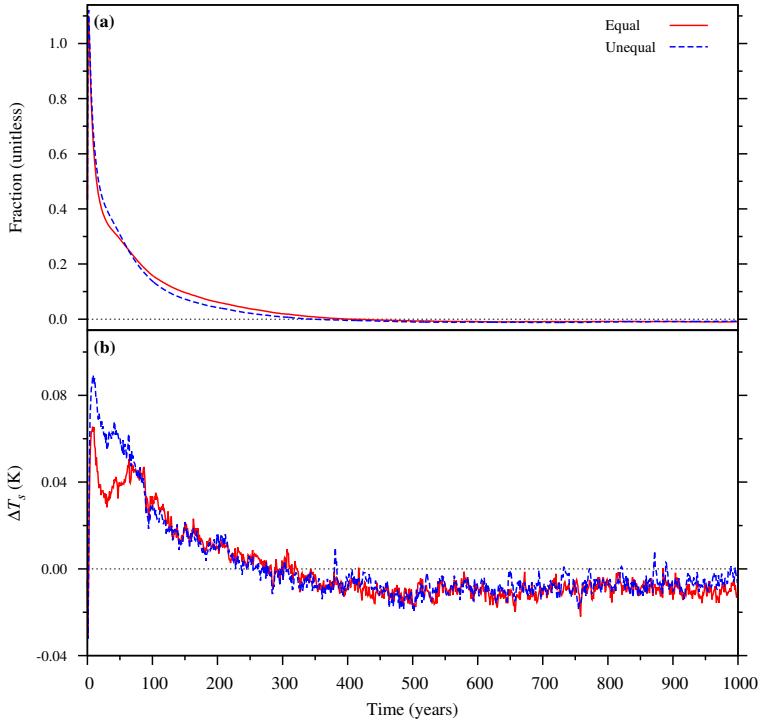

Figure 9. Differences between two distinct spatial patterns of fire pulses both resulting in gross emissions of 100 Pg C. For the "equal" pattern, the burned area fraction was the same in each fire cell. For the "unequal" pattern, the burned area fraction was two times higher between 27° S and 27° N than for other latitudes. **(a)** Airborne fraction of the fire pulse. **(b)** Change in global mean atmospheric surface temperature.